

Achromatic optical Fourier transformer with planar-integrated free-space optics

Gladys Mínguez-Vega, Matthias Gruber, Jürgen Jahns, and Jesús Lancis

We address the problem of achromatization of an optical system for the realization of planar-integrated, free-space optics. In particular we demonstrate an integrated optical Fourier transformation module that was achromatized for the visible spectrum by means of a diffractive lens doublet. The optical system design is studied by using the parabolic approximation of the scalar diffraction theory, including terms related to astigmatism. Based on the method of *ABCD* ray matrices, the optical specifications of the lens doublet are derived and the chromatic correction effect is quantified. For experimental confirmation the diffraction patterns of various grating structures are evaluated. © 2005 Optical Society of America
OCIS codes: 070.2590, 050.1960, 130.3120.

1. Introduction

Planar-integrated, free-space optical (PIFSO) systems are based on miniaturizing and folding conventional free-space optical systems into planar transparent substrates and on fabricating them by means of lithography-based, batch-processing techniques.¹ This provides compatibility with modern (opto)electronics and makes PIFSOS an ideal platform for complex photonic microsystems: Array generators,² optical correlators,³ massively parallel⁴ and vector-matrix-type optical interconnects,^{5,6} wavelength division multiplexers, and demultiplexers⁷ are a few possibilities that this technology may offer for short-range optical communications. Moreover this integration approach can also be made compatible with fiber optics, which is the established technology in the long- and medium-range communication domains.⁸

Although other implementations are conceivable, PIFSOS are often implemented with diffractive optical elements (DOEs) because they provide a large amount of design flexibility and high accuracy achievable with a comparatively low fabrication ef-

fort. Any optical system, however, based on DOEs is subject to the wavelength dependence of free-space propagation.⁹ On the other hand, for many practically important light sources the emission bandwidth is broadband (as in a white-light, light-emitting diode or ultrafast lasers) or the emission wavelength drifts with temperature (as with vertical-cavity surface-emitting lasers). Furthermore some applications require optical systems that can handle a set of different wavelengths. Important examples are wavelength division multiplexers, which are nowadays used extensively to increase bandwidth in communication devices^{7,10} or color processors that exploit, such as human vision, color information from input scenes.¹¹ Recently a method has been presented for designing paraxial-domain diffractive elements working over a broadband frequency range with high efficiency.¹² Remember, however, that the diffraction properties of the field in the region behind the element still remain wavelength dependent.

Earlier work related to the use of PIFSOS with broadband illumination was focused on the fabrication of reflective microlenses by means of e-beam lithography.¹³ These microlenses are concave mirrors with a constant image focal length for all the wavelengths of the source. Therefore these elements are well adapted to broadband imaging purposes. However, even if only DOEs are used in a system, it may be used over a finite wavelength range without significant deterioration in performance. This was analyzed in Ref. 14 and exploited more specifically in Ref. 15 where a white-light holographic doublet was proposed to reconstruct three-dimensional images. In the latter case the spectral selectivity of the first

G. Mínguez-Vega (gminguez@exp.uji.es) and J. Lancis are with the Departament de Ciències Experimentals, Universitat Jaume I, 12071 Castellón, Spain. M. Gruber and J. Jahns are with the FernUniversität Hagen, Lehrgebiet Optische Nachrichtentechnik, Universitätsstrasse 27/Philipp-Reis-Gebäude, 58084 Hagen, Germany.

Received 2 July 2004; revised manuscript received 1 October 2004; accepted 7 October 2004.

0003-6935/05/020229-07\$15.00/0

© 2005 Optical Society of America

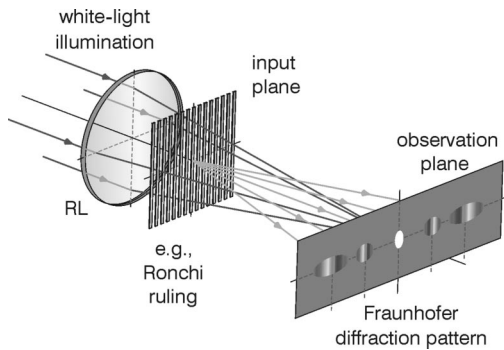


Fig. 1. Conventional setup for implementing an optical Fourier transformation. All diffraction orders except the zeroth order exhibit chromatic dispersion.

hologram was used to select a narrow bandwidth for the display.

A second key function besides imaging that can be carried out optically in interconnection and signal-processing applications is Fourier transformation.¹⁶ A planar-integrated Fourier transformer module without phase errors has been proposed.¹⁷ Owing to the intrinsic properties of the propagation of electromagnetic waves, the Fraunhofer diffraction pattern of an arbitrary diffracting screen illuminated with a broadband source obtained at the back focal plane of an ideal refractive lens (RL) has strong lateral chromatic distortion as shown schematically in Fig. 1. Different methods have been applied in bulk optics to compensate for this chromatic dispersion when all-glass, achromatic, Fourier-transform lenses^{18,19} and combinations of holographic and strongly dispersive refractive elements in cascade are used.²⁰ However, dispersion-compensated Fourier transformers that combine only diffractive lenses and ideal nondispersive refractive objectives are certainly easier to handle.^{21–28}

As a first example of the application of achromatic systems to planar optics we have developed a PIFSO achromatic Fourier transformer (AFT). For our integration purposes the scale-tunable AFT in Refs. 27 and 28 appears to be the most suitable system. In Section 2 we review the main characteristics of the AFT. In Section 3 the design of the PIFSO-AFT module is made into the framework of the parabolic approximation of the scalar diffraction theory applied to tilt the optical axis and is described by the *ABCD* ray matrices. Finally in Section 4 we describe the fabrication characteristics of the achromatic Fourier module and show some experimental results.

2. Achromatic Fourier Transformer in Bulk Optics

The propagation of electromagnetic waves in free space is a physical phenomenon that explicitly depends on the wavelength of light. In an optical Fourier transformer, broadband-dispersion compensation is required if the diffraction pattern must be identical with respect to all the spectral components of the incident light. The compensating procedure lies in achieving an incoherent superposition of the mono-

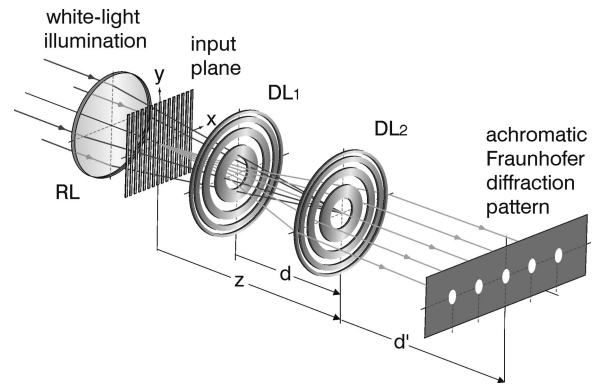


Fig. 2. Addition of a diffractive lens doublet to the setup in Fig. 1 for obtaining an achromatic optical Fourier transformation.

chromatic versions of the Fraunhofer pattern in a single plane and with the same scale for all the temporal components of the source. Achromatic optical Fourier transformers meet the above requirement in a first-order approximation. For white-light illumination all diffraction orders should then, unlike in Fig. 1, appear as well-focused white spots as in Fig. 2.

In general the task of compensating for the dispersion of the diffraction pattern requires optical elements that are themselves dispersive in nature. The AFT is constituted of diffractive lenses (DLs). Since diffractive elements are usually fabricated by binary-optics technology and have a limited diffraction efficiency, it is recommended that their total number be kept as low as possible to minimize the loss. The bulk achromatic Fourier transformer that we adapted to the PIFSO system consists of a diffractive doublet as shown in Fig. 2. The input object is illuminated by a converging beam that has a virtual focus at a distance z from the transparency in the on-axis position of the second DL. DL_1 and DL_2 represent diffractive lenses separated by a distance d . The image focal lengths of DL_1 and DL_2 are $Z_1 = f_1\sigma/\sigma_0$ and $Z_2 = f_2\sigma/\sigma_0$, respectively, where $\sigma = 1/\lambda$ is the wave number. Finally the output plane of the system is located a distance d' from DL_2 and corresponds to the Fraunhofer plane of the setup for the design wave number.

By means of the geometrical-optics description as in Ref. 27 and based on a step-by-step calculation of the Fresnel diffraction integral as in Ref. 28, two system conditions for achieving an achromatic Fraunhofer pattern in irradiance are derived:

$$d = (-f_1f_2)^{1/2}, \quad d' = -\frac{d^2}{d + 2f_1}. \quad (1)$$

Since the achromatic Fourier transformation is achieved in a first-order theory, the proposed setup suffers from residual chromatic aberrations. A good measure of the longitudinal chromatic aberration (LCA) and transversal chromatic aberration (TCA) can be obtained from

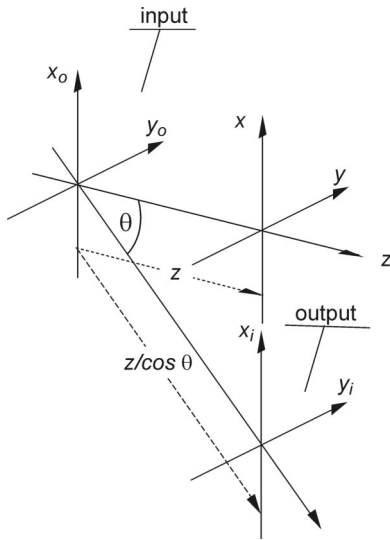


Fig. 3. Definition of the coordinate systems.

$$\begin{aligned} \text{LCA} &= 100 \frac{d'(\sigma_0) - d'(\sigma)}{d'(\sigma_0)}, \\ \text{TCA} &= 100 \frac{x(\sigma_0) - x(\sigma)}{x(\sigma_0)}, \end{aligned} \quad (2)$$

where $d'(\sigma)$ indicates the wavelength-dependent distance from DL_2 to the Fraunhofer plane and $x(\sigma)$ is the scale of the Fourier transform in the x direction for wave number σ . Note that the TCA in the y direction has the same value as in the x direction. These chromatic aberrations, CA, both axial and transversal, have the same value as given by

$$\text{CA} = \frac{100}{1 + \left[2 - \left(\frac{f_2}{f_1} \right)^{1/2} \right] \frac{\sigma_0 \sigma}{(\sigma - \sigma_0)^2}}. \quad (3)$$

Then, with a suitable selection of the ratio between the image focal distances of the DLs and the design wave number, the chromatic aberrations can be reduced to less than 10%. For more detailed information about the AFT, see Refs. 27 and 28.

3. Design of the Planar-Integrated System Version by Use of Ray Matrices

In most applications including this one the Rayleigh-Sommerfeld theory for scalar diffraction can be approximated to reduce the mathematical complexity of the integral expression. It is well known that, with the assumption that the distance between the input and the output planes is larger than their lateral dimensions, the Fresnel approximation for on-axis waves can be used. With this approximation the output amplitude distribution $U(x, y; \sigma)$ in a certain plane z perpendicular to an optical axis, see Fig. 3,

can be calculated from the initial amplitude of a signal, $t(x_0, y_0)$, in the following way:

$$\begin{aligned} U(x, y; \sigma) &= \exp \left[i\pi\sigma \frac{1}{z} (x^2 + y^2) \right] \\ &\times \int_{-\infty}^{\infty} t(x_0, y_0) \exp \left[i\pi\sigma \frac{1}{z} (x_0^2 + y_0^2) \right] \\ &\times \exp \left[-i2\pi\sigma \frac{1}{z} (xx_0 + yy_0) \right] dx_0 dy_0, \end{aligned} \quad (4)$$

where σ is the wave number in the propagation medium and where some irrelevant constant factors have been omitted. Now, if we consider a general optical system with revolution symmetry that is described by a certain $ABCD$ ray matrix corresponding to propagation between the input and the output planes, the Fresnel diffraction integral becomes^{29,30}

$$\begin{aligned} U(x, y; \sigma) &= \exp \left[i\pi\sigma \frac{D}{B} (x^2 + y^2) \right] \\ &\times \int_{-\infty}^{\infty} t(x_0, y_0) \exp \left[i\pi\sigma \frac{A}{B} (x_0^2 + y_0^2) \right] \\ &\times \exp \left[-i2\pi \frac{\sigma}{B} (xx_0 + yy_0) \right] dx_0 dy_0. \end{aligned} \quad (5)$$

One inherent property of planar optical systems is the propagation of light signals along an oblique optical axis tilted by an angle θ that is typically of the order of 10 deg (Fig. 3). In this case the mathematical approximations that lead to Eq. (4) are no longer valid in general, which means that a more sophisticated mathematical treatment is required. By applying the scalar diffraction theory for the case of a paraxial wave propagating along a tilted optical axis and by performing a parabolic approximation in a nonorthogonal coordinate system, we can write the output amplitude distribution in the coordinate system (x_i, y_i) as^{17,31,32}

$$\begin{aligned} U(x_i, y_i; \sigma) &= \exp \left[i\pi\sigma \left(\frac{\cos^3 \theta}{z} x_i^2 + \frac{\cos \theta}{z} y_i^2 \right) \right] \\ &\times \int_{-\infty}^{\infty} t(x_0, y_0) \exp \left[i\pi\sigma \left(\frac{\cos^3 \theta}{z} x_0^2 \right. \right. \\ &\left. \left. + \frac{\cos \theta}{z} y_0^2 \right) \right] \exp \left[-i2\pi\sigma \left(\frac{\cos^3 \theta}{z} x_i x_0 \right. \right. \\ &\left. \left. + \frac{\cos \theta}{z} y_i y_0 \right) \right] dx_0 dy_0. \end{aligned} \quad (6)$$

In this expression the asymmetry between the x_i and y_i coordinate becomes evident. The effects of the astigmatism, because the optical signal and elements in a planar system are not perpendicular to the op-

Table 1. *ABCD* Matrix for an On-Axis System and for Propagation in a Planar-Integrated Device

Elements of the Optical System	Ray Matrix for a System with Revolution Symmetry	Ray Matrix for a Planar System in the x Direction	Ray Matrix for a Planar System in the y Direction
Free-space propagation	$\begin{bmatrix} 1 & z \\ 0 & 1 \end{bmatrix}$	$\begin{bmatrix} 1 & z/\cos^3 \theta \\ 0 & 1 \end{bmatrix}$	$\begin{bmatrix} 1 & z/\cos \theta \\ 0 & 1 \end{bmatrix}$
Refractive lens	$\begin{bmatrix} 1 & 0 \\ -1/f & 1 \end{bmatrix}$	$\begin{bmatrix} 1 & 0 \\ -\cos^3 \theta/f & 1 \end{bmatrix}$	$\begin{bmatrix} 1 & 0 \\ -\cos \theta/f & 1 \end{bmatrix}$
Diffractive lens	$\begin{bmatrix} 1 & 0 \\ -\sigma_0/f_0\sigma & 1 \end{bmatrix}$	$\begin{bmatrix} 1 & 0 \\ -\sigma_0 \cos^3 \theta/f_0\sigma & 1 \end{bmatrix}$	$\begin{bmatrix} 1 & 0 \\ -\sigma_0 \cos \theta/f_0\sigma & 1 \end{bmatrix}$

tical axis, are included in the diffraction integral. Note that for a change of variables $x_0' = x_0 \cos^3 \theta$ and $y_0' = y_0 \cos \theta$ the only difference between the on-axis case is that the output intensity distribution has a scale change between the x_i and the y_i coordinates. This means that, except for a scale factor, we can assume the same kind of intensity diffraction patterns for Eqs. (4), and (6). If we consider now a general optical system, we can also apply the *ABCD* law, but, owing to the asymmetry, we obtain

$$\begin{aligned}
 U(x_i, y_i; \sigma) = & \exp \left[i\pi\sigma \left(\frac{D_x}{B_x} x_i^2 + \frac{D_y}{B_y} y_i^2 \right) \right] \\
 & \times \int_{-\infty}^{\infty} t(x_0, y_0) \exp \left[i\pi\sigma \left(\frac{A_x}{B_x} x_0^2 + \frac{A_y}{B_y} y_0^2 \right) \right] \\
 & \times \exp \left[-i2\pi \left(\frac{\sigma}{B_x} x_i x_0 + \frac{\sigma}{B_y} y_i y_0 \right) \right] dx_0 dy_0.
 \end{aligned} \tag{7}$$

So, a complete description of a planar optical system requires a separate *ABCD* matrix for each direction. Table 1 shows a few examples of elementary ray matrices used for designing planar systems. Note at this point that, because we consider σ the wave number in the propagation medium, the focal length of the diffractive lenses f already corresponds to the glass substrate of the planar optical system.

The design of the PIFSO-AFT module is schematically shown in Fig. 4. An achromatic refractive

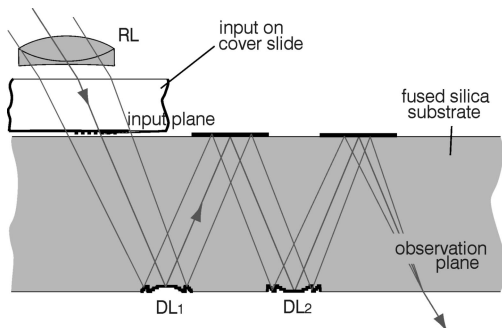


Fig. 4. Cross section of the PIFSO-type achromatic Fourier-transform module.

micro-objective generates the converging beam that illuminates the input object (relayed over the planar substrate). The two diffractive lenses are operated in reflection and integrated on a glass wafer of thickness h . The planar integration restricts the distances between the diffractive elements to a multiple of h . To reduce fabrication complexity it is desirable to integrate all the diffractive lenses on the same side of the substrate.

The *ABCD* matrix of the PIFSO-AFT configuration for the x_i direction corresponds to

$$\begin{aligned}
 \begin{bmatrix} A_x & B_x \\ C_x & D_x \end{bmatrix} = & \begin{bmatrix} 1 & 2h/\cos^3 \theta \\ 0 & 1 \end{bmatrix} \begin{bmatrix} 1 & 0 \\ -\sigma_0 \cos^3 \theta/f_2\sigma & 1 \end{bmatrix} \\
 & \times \begin{bmatrix} 1 & 2h/\cos^3 \theta \\ 0 & 1 \end{bmatrix} \\
 & \times \begin{bmatrix} 1 & 0 \\ -\sigma_0 \cos^3 \theta/f_1\sigma & 1 \end{bmatrix} \\
 & \times \begin{bmatrix} 1 & h/\cos^3 \theta \\ 0 & 1 \end{bmatrix} \begin{bmatrix} 1 & 0 \\ -\cos^3 \theta/3h & 1 \end{bmatrix}.
 \end{aligned} \tag{8}$$

In Eq. (8) the individual matrices have the following meaning (from right to left): a converging source that illuminates the object and focuses over DL_2 , free-space propagation inside the substrate across an effective distance $h/\cos^3 \theta$, the astigmatic diffractive lens DL_1 , a free-space propagation inside the wafer between the two diffractive lenses; the astigmatic diffractive lens DL_2 , and finally a free-space propagation between DL_2 and the output plane.

To achieve an achromatic correction of both the position and scale of the Fraunhofer pattern of the input, according to Eq. (7), the system must accomplish for the x_i direction that

$$A_x|_{\sigma_0} = 0, \quad \left. \frac{\partial}{\partial \sigma} \left(\frac{A_x \sigma}{B_x} \right) \right|_{\sigma_0} = 0, \tag{9a}$$

$$\left. \frac{\partial}{\partial \sigma} \left(\frac{\sigma}{B_x} \right) \right|_{\sigma_0} = 0. \tag{9b}$$

Equations (9a) ensure that the output amplitude distribution of the system for wave number σ_0 is the Fraunhofer pattern of the input and moreover that a stationary value of the quadratic exponential of the Fresnel integral is obtained. Equation (9b) leads to an achromatic correction of the scale factor of the Fourier transformation. Straightforward mathematical calculus leads to the following design conditions for PIFSO-AFT:

$$f_1 = -2h, \quad f_2 = 2h. \quad (10)$$

The two diffractive lenses have to have equal focusing power but with opposite sign. Note that the results in Eq. (10) agree with those given in Eq. (1) after $d = d' = 2h$ is considered.

Similar calculations provide identical relations for the focal length of the DLs in the y_i direction. However, owing to the anamorphic behavior of the system, the scale factor of the Fourier transform is different for each direction. From Eq. (7) the scale factor in the Fraunhofer plane for the design wave number is

$$\frac{x_i}{\mu} = \frac{B_x}{\sigma_0} = \frac{3h}{\sigma_0 \cos^3 \theta}, \quad \frac{y_i}{\nu} = \frac{B_y}{\sigma_0} = \frac{3h}{\sigma_0 \cos \theta}, \quad (11)$$

where μ and ν are the spatial frequencies. This different scale in each direction because of the tilt of the axis was also a point in Ref. 17.

Next we evaluate the chromatic aberrations of the PIFSO-AFT. After considering the definitions provided by Eq. (2), we get

$$CA = LCA = TCA = 100 \frac{(\sigma - \sigma_0)^2}{\sigma^2 - \sigma\sigma_0 + \sigma_0^2}, \quad (12)$$

so both geometrical chromatic errors have identical analytical expressions in agreement with Eq. (3).

4. Practical Implementation and Experiments

The PIFSO-AFT module was fabricated by optical lithography with UV light and reactive ion etching. This ensures precise positioning of all the elements on the glass wafer. With the available equipment, minimum features of $\sim 1 \mu\text{m}$ could be realized. The system was constructed in a quartz glass substrate of thickness $h = 3 \text{ mm}$ and refractive index $n = 1.45$. As the light source a white-light high-pressure mercury arc lamp was used that has substantial light emission throughout the whole visible spectrum. Light was coupled into the setup through a single-mode optical fiber. Figure 5 shows the experimental setup and the quartz substrate; encircled is the PIFSO-AFT that was designed for the visible spectrum.

If we assume a source bandwidth of $\Delta\sigma = 1600 \text{ mm}^{-1}$ centered around a design wave number of $\sigma_0 = 2570 \text{ mm}^{-1}$ (corresponding to 388 nm in a substrate with a refractive index of 1.45), then in accordance with Eq. (12) the chromatic errors are

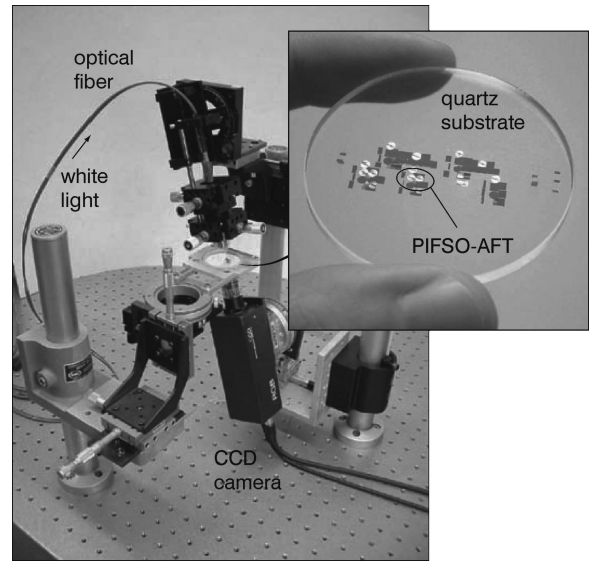


Fig. 5. Experimental setup and quartz glass substrate with the PIFSO-AFT.

$\sim 7\%$. We neglect the refractive-index variation of the wavelength in the spectral range of the broadband source. The angle of light propagation inside the substrate has a nominal value of $\theta = 13.73^\circ$. This provides from Eq. (11) a scale change between the x_i and y_i coordinates of $\cos^2 \theta = 0.94$.

Following Eq. (10) the image focal distances for the four-phase-level DLs etched into the bottom surface of the substrate are $f_2 = -f_1 = 6 \text{ mm}$. A diffractive lens with four phase levels has a theoretical efficiency of approximately 81% for the design wave number. The two lenses used in our setup therefore provide the setup's diffraction efficiency of 65% for σ_0 . If we also consider fabrication errors and losses due to mirrors, the overall efficiency of the system is slightly lower.

In Fig. 6 we present the experimental results obtained with a (black-and-white) CCD camera and the architecture of Fig. 4. As input objects two different binary amplitude patterns on microscopic cover slides are used. The first is a computer-generated hologram (CGH) designed by an iterative Fourier-transform algorithm. The hologram produces a star-like image in the Fourier plane. The upper row in Fig. 6 corresponds to the star CGH. Figure 6(a) shows the irradiance observed in the Fourier plane when light passes through a substrate composed only of mirrors, thus corresponding to the setup in Fig. 1. Figure 6(b) shows the situation with the PIFSO-AFT module.

The second is a regular Ronchi ruling. It is well known that the Fourier transform of the amplitude transmittance of the grating consists of a discrete series of diffraction orders. The lower row in Fig. 6 shows the respective results for the Ronchi ruling together with the linear intensity scans across the center of the peaks. The achromatization effect is obvious, especially from a comparison of the third diffraction orders of the Ronchi ruling. In Fig. 6(d) the

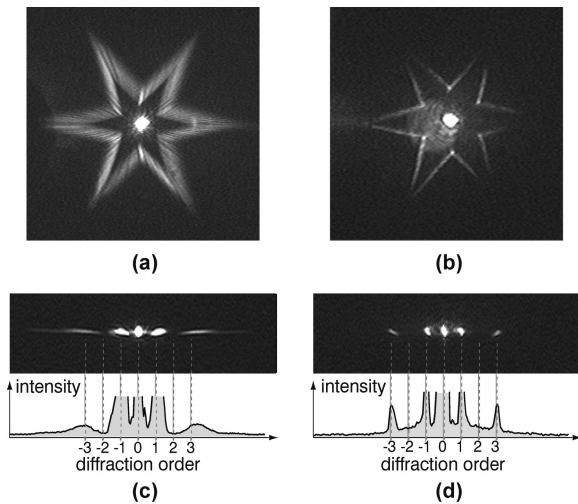


Fig. 6. CCD images (left column) showing experimental results obtained with a PIFSO version of the conventional Fourier-transform setup of Fig. 1 for (a) a CGH and (c) a Ronchi grating. The images in the right column correspond to the PIFSO-AFT in Fig. 4 and show results obtained with the same objects.

diffraction spot is spatially well confined, whereas it is smeared in Fig. 6(c).

These experimental results show the validity of our PIFSO-AFT in working with broadband light for image processing or an optical interconnection. The only attention that must be given to data-processing applications is the scale change of the Fourier transform for each direction.

5. Conclusions

We have demonstrated theoretically and experimentally the implementation of an achromatic Fourier transformer in a planar-optics configuration. In this way we can overcome one of the greatest drawbacks of planar-integrated Fourier modules illuminated with broadband light, the chromatic aberration obtained in the Fraunhofer pattern owing to the wavelength dependence of free-space propagation.

We have exploited the chromatic aberration associated with diffractive lenses to fabricate the PIFSO-AFT module. The study of light propagation through the planar system has been carried out in the framework of the scalar diffraction theory in terms of the $ABCD$ matrices for the tilt axis devices. This allows us to obtain design constraints for the setup. Note that the PIFSO-AFT is an anamorphic system so that the Fourier transformation provides a different magnification in the x and y direction.

Furthermore the validity of the setup was experimentally evaluated by the realization of the achromatic Fourier transformation of a CGH and a one-dimensional Ronchi grating with white light. Studies to increase the integration ability of the system are currently on going.

This research was done at the Optische Nachrichtentechnik-group at the FernUniversität Hagen, Germany. G. Mínguez-Vega gratefully ac-

knowledges financial support from the Generalitat Valenciana, Agencia Valencia de Ciencia y Tecnología (grant CTESPP/2003/068). She also thanks P. Andrés for useful discussions of the achromatic Fourier transformer in bulk optics.

References

1. J. Jahns and A. Huang, "Planar integration of free-space optical components," *Appl. Opt.* **28**, 1602–1605 (1989).
2. M. M. Downs and J. Jahns, "Integrated-optical array generator," *Opt. Lett.* **15**, 769–770 (1990).
3. W. Eckert, V. Arrizon, S. Sinzinger, and J. Jahns, "Compact planar-integrated optical correlator for spatially incoherent signals," *Appl. Opt.* **39**, 759–765 (2000).
4. S. Sinzinger and J. Jahns, "Integrated micro-optical imaging system with a high interconnection capacity fabricated in planar optics," *Appl. Opt.* **36**, 4729–4735 (1997).
5. M. Gruber, S. Sinzinger, and J. Jahns, "Planar-integrated optical vector-matrix multiplier," *Appl. Opt.* **39**, 5367–5373 (2000).
6. M. Gruber, "Multichip module with planar-integrated free-space optical vector-matrix-type interconnects," *Appl. Opt.* **43**, 463–470 (2004).
7. R. Shechter, Y. Amitai, and A. A. Friesem, "Compact wavelength division multiplexers and demultiplexers," *Appl. Opt.* **41**, 1256–1261 (2002).
8. M. Gruber, E. El Joudi, S. Sinzinger, and J. Jahns, "Practical realization of massively parallel fiber-free-space optical interconnects," *Appl. Opt.* **40**, 2902–2908 (2001).
9. T. Stone and N. George, "Wavelength performance of holography optical elements," *Appl. Opt.* **24**, 3797–3810 (1985).
10. E. A. De Souza, M. C. Nuss, W. H. Knox, and D. A. B. Miller, "Wavelength-division multiplexing with femtosecond pulses," *Opt. Lett.* **20**, 1166–1168 (1995).
11. P. Andrés, V. Climent, J. Lancis, G. Mínguez-Vega, E. Tajahuerce, and A. W. Lohmann, "All-incoherent dispersion-compensated optical correlator," *Opt. Lett.* **24**, 1331–1333 (1999).
12. H. Lajunen, J. Tervo, and J. Turunen, "High-efficiency broadband diffractive elements based on polarization grating," *Opt. Lett.* **29**, 803–805 (2004).
13. T. Shiono and H. Ogawa, "Reflection aspherical microlenses for planar optics fabricated by electron-beam lithography," *Opt. Lett.* **17**, 565–567 (1992).
14. J. Jahns, Y. H. Lee, Ch. A. Burrus, and J. L. Jewell, "Optical interconnects using planar optics and microlasers," *Appl. Opt.* **31**, 592–597 (1992).
15. Y. Amitai, I. Shariv, M. Kroch, A. A. Friesem, and S. Reinhorn, "White-light holographic display based on planar optics," *Opt. Lett.* **18**, 1265–1267 (1993).
16. F. T. S. Yu and S. Jutamulia, *Optical Pattern Recognition* (Cambridge University, New York, 1998).
17. S. Reinhorn, S. Gorodeisky, A. A. Friesem, and Y. Amitai, "Fourier transformation with a planar holographic doublet," *Opt. Lett.* **20**, 495–497 (1995).
18. C. G. Wyne, "Extending the bandwidth of speckle interferometry," *Opt. Commun.* **28**, 21–25 (1979).
19. C. Brophy, "Design of an all-glass achromatic Fourier transform lens," *Opt. Commun.* **47**, 364–368 (1983).
20. G. M. Morris, "Diffraction theory for an achromatic Fourier transformation," *Appl. Opt.* **20**, 2017–2025 (1981).
21. R. H. Katyl, "Compensating optical systems. Part 3: Achromatic Fourier transformation," *Appl. Opt.* **11**, 1255–1260 (1972).
22. R. Ferrière and J. P. Goedgebuer, "Achromatic systems for far-field diffraction with broadband illumination," *Appl. Opt.* **22**, 1540–1545 (1983).

23. P. Andrés, J. Lancis, and W. D. Furlan, "White-light Fourier transformer with low chromatic aberration," *Appl. Opt.* **23**, 4682–4687 (1992).
24. M. Schwab, N. Lindlein, J. Schwider, Y. Amitai, A. A. Friesem, and S. Reinhorn, "Compensation of the wavelength dependence in diffractive star couplers," *J. Opt. Soc. Am. A* **12**, 1290–1297 (1995).
25. J. Lancis, E. Tajahuerce, P. Andrés, G. Mínguez-Vega, M. Fernández-Alonso, and V. Climent, "Quasi-wavelength-independent broadband optical Fourier transformer," *Opt. Commun.* **172**, 153–160 (1999).
26. D. Wang, A. Pe'er, A. W. Lohmann, and A. A. Friesem, "Wigner algebra as a tool for the design of achromatic optical processing systems," *Opt. Eng.* **39**, 3014–3024 (2000).
27. J. Lancis, P. Andrés, W. D. Furlan, and A. Pons, "All-diffractive achromatic Fourier-transform setup," *Opt. Lett.* **19**, 402–404 (1994).
28. E. Tajahuerce, V. Climent, J. Lancis, M. Fernández-Alonso, and P. Andrés, "Achromatic Fourier transforming properties of a separated diffractive lens doublet: theory and experiment," *Appl. Opt.* **37**, 6164–6173 (1998).
29. A. E. Siegman, *Lasers* (University Science, Mill Valley, Calif., 1986).
30. F. L. Pedrotti and L. S. Pedrotti, *Introduction to Optics* (Prentice-Hall, Englewood Cliffs, N.J., 1993).
31. M. Testorf and J. Jahns, "Paraxial theory of planar integrated systems," *J. Opt. Soc. Am. A* **14**, 1569–1575 (1997).
32. M. Testorf and J. Jahns, "Imaging properties of planar-integrated micro-optics," *J. Opt. Soc. Am. A* **16**, 1175–1183 (1999).